

Uncovering Hidden Connections: Iterative Tracking and Reasoning for Video-grounded Dialog

Haoyu Zhang, Meng Liu, *Member, IEEE*, Yaowei Wang, *Member, IEEE*, Da Cao, Weili Guan, *Member, IEEE*, Liqiang Nie, *Senior Member, IEEE*

Abstract—In contrast to conventional visual question answering, video-grounded dialog necessitates a profound understanding of both dialog history and video content for accurate response generation. Despite commendable strides made by existing methodologies, they often grapple with the challenges of incrementally understanding intricate dialog histories and assimilating video information. In response to this gap, we present an iterative tracking and reasoning strategy that amalgamates a textual encoder, a visual encoder, and a generator. At its core, our textual encoder is fortified with a path tracking and aggregation mechanism, adept at gleaning nuances from dialog history that are pivotal to deciphering the posed questions. Concurrently, our visual encoder harnesses an iterative reasoning network, meticulously crafted to distill and emphasize critical visual markers from videos, enhancing the depth of visual comprehension. Culminating this enriched information, we employ the pre-trained GPT-2 model as our response generator, stitching together coherent and contextually apt answers. Our empirical assessments, conducted on two renowned datasets, testify to the prowess and adaptability of our proposed design.

Index Terms—Video-grounded Dialog, Path Tracking, Iterative Reasoning.

1 INTRODUCTION

WITH the rapid proliferation of multimedia data, research attention has intensified on visual-language tasks, attesting to their pivotal role in academic research [1]–[3]. Notable advancements have been realized in fields such as Visual Question Answering (VQA) [4], [5], Visual Dialog [6], [7], and Video Captioning [8], [9]. Central to these tasks is the aim to refine machine capabilities in understanding visual content and to convey these understandings linguistically in ways intelligible to humans.

An emerging domain of significance is video-grounded dialog¹, sometimes referred to as audio-visual scene-aware dialog by certain academicians [10]–[13]. As illustrated in Figure 1, this rapidly evolving domain mandates the creation of an agent adept at conducting coherent dialogs rooted in video data, which is a monumental leap toward

genuine human-computer synergy. The ramifications of video-grounded dialog are broad, spanning enhancements in virtual personal assistants to innovations tailored for visually impaired individuals, thereby underlining its academic importance. Spurred by advancements in deep learning, the domain of video-grounded dialog is witnessing considerable traction. Existing techniques within this sphere can be methodically categorized into:

1) **Textual Information Modeling.** This branch emphasizes modeling textual elements, predominantly involving dialog inquiries and their preceding contexts [14]–[16]. For instance, Le *et al.* [15] devised a semantic graph anchored in the lexical components of Q&A pairs, leading to a model proficient in forecasting reasoning pathways on the graph. This methodology is adept at extracting question-specific data from dialogic contexts. In a related development, Kim *et al.* [14] employed the Gumbel-Softmax technique to identify dialog history utterances that are most pertinent to a given question, enhancing question representations in the process.

2) **Visual Information Modeling.** This avenue of inquiry highlights visual elements, primarily focusing on video frames and notable objects [17]–[20]. As a case in point, Le *et al.* [18] propounded a bidirectional model that encapsulates both spatial-to-temporal relations and their converse, aiming to harness the intricate spatial and temporal subtleties embedded in video. Concurrently, Geng *et al.* [17] advocated representing videos via spatio-temporal scene graphs, capturing salient audio-visual cues and their semantic interrelations effectively.

3) **Decoder Generation.** This frontier emphasizes the formulation of answer derivations [21]–[23]. Noteworthy is Le *et al.* [22] extending the established functionalities of the

- Haoyu Zhang is with the School of Computer Science and Technology, Harbin Institute of Technology (Shenzhen Campus), Shenzhen 518055, China, and also with Peng Cheng Laboratory, Shenzhen 518066, China (e-mail: zhang.hy.2019@gmail.com).
- Meng Liu is with the School of Computer Science and Technology, Shandong Jianzhu University, Jinan 250101, China (e-mail: mengliu.sdu@gmail.com).
- Yaowei Wang is with the Peng Cheng Laboratory, Shenzhen 518066, China (e-mail: wangyw@pcl.ac.cn).
- Da Cao is with the School of Computer Science and Electronic Engineering, Human University, Changsha 410082, China (e-mail: caoda0721@gmail.com).
- Weili Guan is with the Faculty of Information Technology, Monash University (Clayton Campus), Melbourne, VIC 3800, Australia, and also with the Peng Cheng Laboratory, Shenzhen 518066, China (e-mail: honeyguan@gmail.com).
- Liqiang Nie is with the School of Computer Science and Technology, Harbin Institute of Technology (Shenzhen Campus), Shenzhen 518055, China (e-mail: nieliqiang@gmail.com).

Corresponding author: Meng Liu and Liqiang Nie.

1. <https://video-dialog.com/>

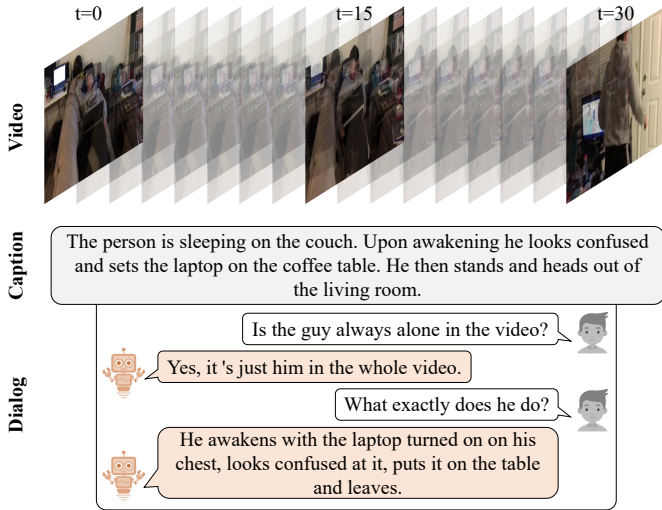


Fig. 1. An illustration of video-grounded dialog.

GPT-2 architecture, eschewing conventional auto-regressive decoding strategies. Complementing this domain, the integration of pointer networks [21] has amplified the generative prowess of dialog systems.

Despite the significant progress observed in the domain of video-grounded dialog, there remain pressing challenges warranting meticulous consideration: 1) **Dialog History Understanding**. Notable recent studies [15], [16] predominantly focus on dialog history segments that align directly with user queries. Such a concentrated perspective can inadvertently exclude broader dialog contexts, leading to the omission of significant information. The inherent lack of transparency in these methods further impedes a clear understanding of the decision-making process of the model. The imperative, therefore, is to develop a superior textual encoder, adept at a comprehensive examination of dialog histories while enhancing model interpretability. 2) **Visual Content Understanding**. While several works [17] endeavor to encapsulate visual signals through complex graph structures, the critical function of user-posed questions in steering visual comprehension is frequently disregarded. This omission leads to a failure to capture question-specific insights, thereby limiting the capacity to mine meaningful visual information. Additionally, the current trend of depending solely on a singular extraction process [19], [20] may be inadequate given the multi-faceted nature of video data. Therefore, an approach that harmonizes user queries with iterative reasoning is crucial for a nuanced comprehension of visual content.

In response to the outlined challenges, we introduce the Iterative Tracking and Reasoning (ITR) framework for video-grounded dialog, detailed in Figure 2. This novel approach aims to redress the limitations of current methodologies by integrating an explicit history modeling mechanism alongside an iterative reasoning strategy. To be specific, we adopt a transparent path tracking and aggregation mechanism, adept at assembling salient information germane to user queries. Such a system amplifies query understanding by sourcing pivotal contextual elements from the dialog history. Concurrently, to harness the latent visual semantics in videos, a multimodal iterative reasoning network is devised. This architecture enables robust

iterative reasoning processes, progressively refining the apprehension of visual content and consequently bolstering generation prowess. The prowess of the ITR paradigm is corroborated through rigorous empirical evaluations on two benchmark datasets. Experimental findings accentuate the proficiency of our framework in obviating the limitations intrinsic to prevailing strategies, thereby achieving state-of-the-art performance. To advance collaborative research, the codebase for the ITR framework is now available at <https://github.com/Hyu-Zhang/ITR>.

The contributions of our work can be highlighted in threefold:

- We present a novel approach for video-grounded dialog that synergizes the modeling of dialog history and visual content into an integrated framework. This harmonization enhances the quality and accuracy of dialog generation.
- We design an explicit path tracking and aggregation system. This methodology enables the effective extraction of vital information from previous dialog interactions, thereby fostering a nuanced understanding of user queries.
- We devise a multimodal iterative reasoning network that leverages user questions. This feature serves to incrementally refine the comprehension of visual content, leading to more precise and context-aware dialog generation.

2 RELATED WORK

2.1 Visual Dialog

Visual dialog represents a sophisticated extension of the VQA framework, requiring multiple rounds of sequential interactions. The fundamental goal of this paradigm is to facilitate a flawless amalgamation of cross-modal information derived from various inputs, culminating in the formation of a coherent textual response. Current methodologies operating within this sphere may be broadly grouped into three distinct paradigms: attention mechanism-based strategies, graph network-based techniques, and approaches reliant on pre-trained models.

Attention Mechanism-based Approaches. These methodologies deploy attention mechanisms to pinpoint the visual regions that bear the highest relevance to the posed question. The underlying process requires an acute understanding of the immediate context of the inquiry, as well as an insight into the historical dialog trajectory. A salient example of this approach is the Recursive visual Attention (RvA) model, formulated by Niu *et al.* [24]. Through iterative refinement of visual attention and retrospective analysis of dialog sequences, this model adeptly addresses co-referential ambiguities. Further complementing this area, Yang *et al.* [25] have innovated two Sequential Dialog Networks (SeqDialN). These networks artfully separate the complexity inherent in multimodal feature fusion from the inference process, thereby simplifying the design and implementation of the inference engine.

Graph Network-based Techniques. Recognizing the pivotal role of seamless information integration, the academic community is incrementally gravitating toward

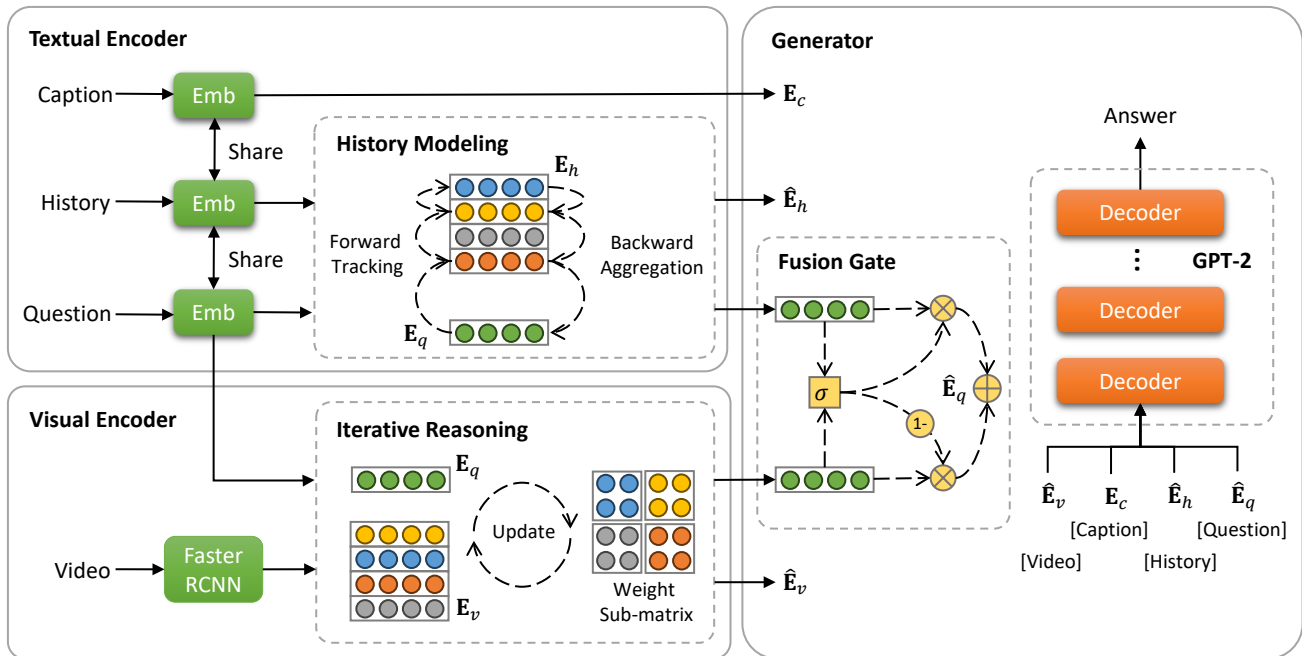


Fig. 2. Illustration of our proposed framework.

graph network methodologies [26]. For instance, Schwartz *et al.* [27] brought forth the Factor Graph Attention (FGA) architecture. This methodology enables the meticulous construction of graphs atop utility representations, subsequently discerning their interconnections. In a parallel vein, Guo *et al.* [28] introduced the Context-Aware Graph (CAG) neural structure, characterized by the dynamic interdependencies exhibited by individual nodes within the graph. Uniquely, this paradigm ensures that only nodes bearing the utmost relevance are integrated, yielding a refined, context-sensitive relational graph logic.

Pre-trained Model-dependent Methods. The contemporary epoch of machine learning has been marked by the ascent of pre-trained models, lauded for their adeptness in seamlessly integrating diverse informational modalities. Anchoring on this insight, Wang *et al.* [29] delineated a holistic strategy that harnesses pre-trained architectures to adroitly weave together visual and dialogical elements. Mirroring this trajectory, Nguyen *et al.* [30] unveiled the Light-weight Transformer for Many Inputs (LTMI), a pioneering neural construct that leans on an agile transformer mechanism to masterfully orchestrate interactions across multifarious utilities.

However, the nuances and complexities of video-grounded dialog tasks preclude the direct application of methodologies cultivated for image-based visual dialog. Video-grounded dialog manifests longer utterance sentences, additional dialog rounds, and a more intricate context that demands sophisticated comprehension [31]. These attributes compound the challenge, rendering the direct transposition of existing visual dialog techniques impractical and inefficacious.

2.2 Video-grounded Dialog

In recent years, the academic community has observed an escalating focus on video-grounded dialog systems. Note-

worthy challenges, including DSTC7 [31] and DSTC8 [32], have been instrumental in formulating benchmarks in this domain. This burgeoning field has subsequently witnessed the advent of numerous sophisticated methodologies to address its inherent complexities. For example, Hori *et al.* [10] pioneered an approach employing an LSTM-driven encoder-decoder framework, placing emphasis on multimodal attention to harmoniously integrate textual and visual cues. Expanding on this work, Le *et al.* [11] presented the Multimodal Transformer Network (MTN), devised specifically to encode visual content while concurrently integrating diverse data modalities. Similarly, innovative contributions like the Bi-directional Spatio-Temporal reasoning model (BiST) [18] have made strides in extracting both visual and spatial cues from videos, thus elucidating the interconnectedness of text and visual sequences in multidimensional aspects. In pursuit of refining co-referential understanding, Kim *et al.* [14] introduced the Structured Co-reference Graph Attention model (SCGA), laying the foundation for a graph-based approach deeply rooted in multimodal co-referencing techniques. In tandem with this, Geng *et al.* [17] advanced the Spatio-Temporal Scene Graph Representation learning technique (STSGR)—an innovative proposition capturing the semantic crux of videos through scene graphs, all the while maintaining efficient encoding.

The ascendance of pre-trained language models in myriad natural language processing domains is unmistakable. Recent efforts are directed towards fusing these models with video-grounded dialog systems. To this end, Le *et al.* [22] advanced the VGD-GPT framework, leveraging the capabilities of the well-regarded GPT-2 model, thus transforming video-grounded dialog generation into a more fluid sequence-to-sequence task. Building on this progression, Li *et al.* [12] incorporated a multi-task learning approach with pre-existing language models, culminating in the inception of the Response Language Model (RLM). Recognizing the

hurdles of text hallucination in text generation, Yoon *et al.* [23] crafted the Text HallucinAtion Mitigating (THAM) architecture, integrating Text Hallucination Regularization (THR) loss into expansive pre-trained language models. In a stride towards achieving nuanced dialog generation, Zhao *et al.* [33] advocated for a Multi-Agent Reinforcement Learning (MARL) methodology, accentuating sophisticated collaborations in cross-modal analysis. With the advent of Large Language Models, such as Video-LLaMA [34] and Otter [35], it is evident that this intricate domain continues to be at the forefront of research attention.

To sum up, within the domain of history modeling, a prevailing trend involves the deployment of intricate graph networks to discern semantic nuances intertwined within historical data. However, these methods often compromise on interpretability. In contrast, our approach embraces a streamlined path tracking and aggregation mechanism, offering superior interpretability. Additionally, current methodologies largely overlook the iterative interplay between videos and questions. We address this oversight, devising an innovative iterative reasoning network that prioritizes this symbiotic relationship.

3 METHODOLOGY

As illustrated in Figure 2, our model consists of three components: a textual encoder, a visual encoder, and a generator. The textual encoder is designed to perform interactions between questions and history contexts and output enhanced representations. Meanwhile, the visual encoder is utilized to implement progressive reasoning between questions and videos, enhancing video content comprehension. Finally, the generator combines multiple input representations to produce system answers. In the following sections, we will elaborate on each component in detail.

3.1 Problem Formulation

The task of video-grounded dialog centers on generating a relevant response A_t in answer to a given question Q_t . This response is derived through a thorough analysis of a video V , a caption C crafted by a human to describe the video, and its associated dialog history H . The dialog history H comprises a series of prior questions and their answers, denoted as (Q_i, A_i) for each i ranging from 1 to $t-1$. Specifically, H is articulated as $\{(Q_1, A_1), \dots, (Q_{t-1}, A_{t-1})\}$. The holistic consideration of these elements is crucial to successfully address the posed question.

3.2 Textual Encoder

3.2.1 Preprocessing

The word embeddings for the given question Q_t , the caption C , and the dialog history H are procured via a consistent mechanism. To elucidate, let's consider the question $Q_t = \{w_1, w_2, \dots, w_{n_q}\}$ as an example. Here, an operation f is applied to the vocabulary obtained from the word-to-id mapping function, $\text{Vocab}(\cdot)$. This process is represented by the following expression:

$$\mathbf{E}_q = f(\text{Vocab}(w_1, w_2, \dots, w_{n_q})), \quad (1)$$

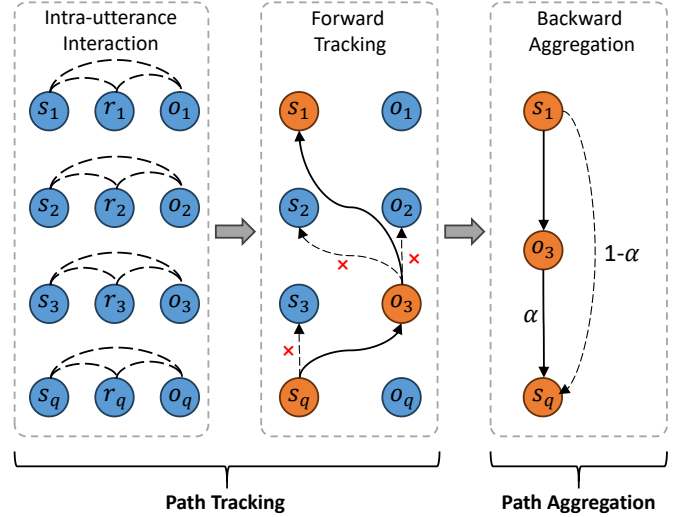


Fig. 3. Illustration of our path tracking and aggregation mechanism.

where $\mathbf{E}_q \in \mathbb{R}^{n_q \times d}$ signifies the resulting word embeddings of the question. The function f corresponds to retrieving the embedding vector associated with the id from the pre-established embedding matrix. The same technique is applied to ascertain the feature of the caption and the dialog history, symbolized as $\mathbf{E}_c \in \mathbb{R}^{n_c \times d}$ and $\mathbf{E}_h \in \mathbb{R}^{(t-1) \times n_h \times d}$, wherein n_c and n_h respectively designates the number of words present in the caption and each utterance.

To bolster the interpretability of questions drawn from the dialog history², we introduce two preprocessing steps: co-reference resolution and dependency parsing. Initially, the dialog history is integrated with the present question to create a unified sequence. We then utilize the AllenNLP³ toolkit for co-reference resolution, aiming to dispel potential confusion related to pronouns. Following this, the Stanford CoreNLP utility⁴ is employed to derive the dependency parse tree. Our attention is concentrated on the dialog history responses due to the inherent similarities between questions and their corresponding answers. This tree delineates the syntactic relationships between sentence constituents. By harnessing the subject-verb-object paradigm, we craft pertinent triplets in the $\langle \text{subject}, \text{relation}, \text{object} \rangle$ format. This conversion facilitates the representation of both the question and dialog history as sets of triplet pairs, denoted as $\mathbf{E}_{tri} \in \mathbb{R}^{t \times 3 \times d}$.

Utilizing the triplet pairs, \mathbf{E}_{tri} , as delineated in the preceding section, we introduce a novel path tracking and aggregation mechanism. This methodology is graphically showcased in Figure 3 and methodologically detailed in Algorithm 1. At its core, this mechanism is designed to cultivate a sophisticated interplay between the question and the dialog history. Notably, it is proficient in extracting pivotal semantic nuances from the dialog history, which subsequently enriches the representation of the question. This process is orchestrated through two consecutive phases: path tracking and path aggregation.

2. Given that the caption inherently encapsulates the essential information, it is utilized directly in the decoding generation process without necessitating further operations.

3. <https://allennai.org/allennlp>.

4. <https://stanfordnlp.github.io/CoreNLP/>.

3.2.2 Path Tracking

The objective of this phase is to meticulously formulate two discrete entity paths, namely the subject and object paths. These carefully constructed paths encompass entities derived from the dialog history, and these entities bear a substantial resemblance to the corresponding subject and object entities present in the question. This complex process is achieved through two principal sub-processes: intra-utterance interaction and forward tracking, each playing a vital role in the coherence and relevance of the entity paths.

(1) Intra-utterance Interaction. To achieve a robust representation of features, it is imperative to incorporate the co-occurrence information of words, serving as an enabling factor for the subsequent forward tracking step. The refinement of the feature pertaining to the subject in the question is governed by the equation:

$$\bar{\mathbf{E}}_{tri}[t][0] = \mathbf{E}_{tri}[t][0] + \text{AvgPool}(\mathbf{E}_{tri}[t][0 : 2]), \quad (2)$$

where $\mathbf{E}_{tri}[t][0]$, $\mathbf{E}_{tri}[t][1]$, and $\mathbf{E}_{tri}[t][2]$ represent the feature of the subject, relation, and object in the question, respectively. The operation $\text{AvgPool}(\cdot)$ signifies the average pooling mechanism. The term $\bar{\mathbf{E}}_{tri}[t][0]$ captures the enhanced feature of the subject entity embedded within the question. An analogous process yields the enhanced feature for the object entity, epitomized by $\bar{\mathbf{E}}_{tri}[t][2]$. By implementing these computational steps on the triplet details spanning all dialog histories $\mathbf{E}_{tri} \in \mathbb{R}^{t \times 3 \times d}$, we derive the refined triplet representation, expressed as $\bar{\mathbf{E}}_{tri} \in \mathbb{R}^{t \times 3 \times d}$.

(2) Forward Tracking. In this phase, our focus shifts towards the execution of the forward tracking sub-process, designed to delineate both the subject path and the object path. To offer clarity, we elucidate the mechanism underpinning the establishment of the subject path. For the subject immanent in the question (*i.e.*, the t -th utterance), we quantify its similarity with the subject and object entities nestled within the $(t-1)$ -th utterance. The decision criterion is encapsulated by the following mathematical formulation:

$$\begin{cases} S[t-1, j/2] = 1, & \text{if } \epsilon_j > p, \\ S[t-1, j/2] = 0, & \text{otherwise,} \end{cases} \quad (3)$$

where ϵ_j represents the similarity score bridging the subject entity in the question and the j -th entity in the $(t-1)$ -th utterance. The symbol p denotes a predetermined selection threshold, while $S \in \mathbb{R}^{(t-1) \times 2}$ is an adjacency matrix. Note that if both entities in the $(t-1)$ -th utterance are larger than p , we choose the larger one, as shown in Algorithm 1. The criterion $S[t-1, j/2] = 1$ indicates that the j -th entity in the $(t-1)$ -th utterance resonates with the subject entity in the question. Hence, the aforementioned j -th entity is appointed as a pivotal point for the ensuing forward comparison.

Furthermore, it is prudent to evolve from the rudimentary comparison feature, namely the feature of the subject in question $\bar{\mathbf{E}}_{tri}[t][0]$. We propose a more advanced comparison feature, denoted by \mathbf{h} , which is structured as:

$$\mathbf{h} = f_t(\bar{\mathbf{E}}_{tri}[t-1][j] || \bar{\mathbf{E}}_{tri}[t][0]), \quad (4)$$

where $\bar{\mathbf{E}}_{tri}[t][0]$ and $\bar{\mathbf{E}}_{tri}[t-1][j]$ designate the feature of the subject entity in the question and the j -th entity (subject or object entity) in the $(t-1)$ -th utterance that correlates with

Algorithm 1 The path tracking and aggregation mechanism

Input: The representation of triplet pairs \mathbf{E}_{tri}

Output: The context-enhanced question representation

\mathbf{E}_q^{txt} and dialog history representation $\hat{\mathbf{E}}_h$

- 1: Establish effective representation $\bar{\mathbf{E}}_{tri}$ by Eqn. (2)
- 2: Initialize adjacency matrix S , comparison feature \mathbf{h}
- 3: **for** $i \leftarrow \{0, 2\}$ **do**
- 4: comparison point (t, i) , $\mathbf{h} = \bar{\mathbf{E}}_{tri}[t][i]$
- 5: **while** $\tau \leftarrow (t-1)$ **to 1 do**
- 6: $\epsilon_0 = \text{Cos}(\mathbf{h}, \bar{\mathbf{E}}_{tri}[\tau][0])$
- 7: $\epsilon_2 = \text{Cos}(\mathbf{h}, \bar{\mathbf{E}}_{tri}[\tau][2])$
- 8: **if** $\epsilon_0 > p$ or $\epsilon_2 > p$ **then**
- 9: $j = \text{argmax}(\epsilon_0, \epsilon_2)$
- 10: comparison point (τ, j)
- 11: $S[\tau, j/2] = 1$, $\mathbf{h} = \bar{\mathbf{E}}_{tri}[\tau][j]$
- 12: **end if**
- 13: **end while**
- 14: **end for**
- 15: **for** $i \leftarrow 1$ **to** t **do**
- 16: Obtain $\mathbf{E}_{tri}^{txt}[i][0]$ and $\mathbf{E}_{tri}^{txt}[i][2]$ based on matrix S by Eqn. (5)
- 17: **end for**
- 18: Output question representation \mathbf{E}_q^{txt} and dialog history representation $\hat{\mathbf{E}}_h$

the subject entity in the question, respectively. The concatenation operation is symbolized by $||$, while f_t denotes a fully connected layer, and \mathbf{h} represents the freshly synthesized feature for the ensuing round of comparison.

By perpetuating the forward comparison until reaching the inception of the dialog, a subject path rooted in the subject entity in the question is formulated. A parallel procedure leads to the creation of the corresponding paths, encompassing both the subject and object paths.

3.2.3 Path Aggregation

In this section, we elaborate on the aggregation mechanism designed to harness the extracted entity paths. The overarching goal is to synthesize a more refined textual representation that encapsulates the crux of the dialog. To achieve this, additional connections are instantiated during the backward traversal of the path, considering the inherent relationships between words. This process has been visually elucidated in Figure 3.

Our strategy leverages an attention mechanism [36], ensuring that during the aggregation process, every node accumulates information from its subsequent nodes, thus refining its representation. For a clearer understanding, let's consider the case of refining the i -th ($i \in \{0, 2\}$) entity in the question. Its updated representation is computed as follows:

$$\begin{cases} \mathbf{E}_{tri}^{txt}[t][i] = \bar{\mathbf{E}}_{tri}[t][i] + \sum_{j \in \mathcal{N}_i} \alpha_{i,j}^{t,k} \mathbf{W}_1 \mathbf{E}_{tri}^{txt}[k][j], \\ \alpha_{i,j}^{t,k} = \text{Softmax}(\gamma_{i,j}^{t,k} + 1/(t-k)), \\ \gamma_{i,j}^{t,k} = \bar{\mathbf{E}}_{tri}^T[t][i] \mathbf{W}_1 \mathbf{E}_{tri}^{txt}[k][j], \end{cases} \quad (5)$$

where $\bar{\mathbf{E}}_{tri}[t][i]$ represents the feature of the i -th entity in the t -th utterance (the current question), while \mathcal{N}_i embodies the set of nodes connected to the i -th entity, *i.e.*, all nodes on the same path. Moreover, $\mathbf{E}_{tri}^{txt}[k][j]$ signifies the updated

feature with aggregated antecedent information of the j -th neighboring entity in the k -th utterance. The matrix \mathbf{W}_1 functions as a parameter matrix used for transformation purposes, and $\mathbf{E}_{tr_i}^{txt}[t][i]$ connotes the updated feature of the i -th entity. An essential aspect of our strategy involves incorporating the distance between utterances into the computation of attention weights. Iteratively applying this mechanism across utterances (from 1 to t) ensures that each entity feature is enhanced. It is worth noting that for nodes with zero in-degree, *e.g.*, entities in the first utterance, we retain their original features.

Following these systematic stages, we derive a richer question representation denoted as $\mathbf{E}_q^{txt} \in \mathbb{R}^{n_q \times d}$. It is worth noting that \mathbf{E}_q^{txt} is constructed by substituting the original word features \mathbf{E}_q with the newly refined features from the triplet pairs while leaving word features from other positions intact. Moreover, the word features in the triplet pairs, represented as $\mathbf{E}_{tr_i}^{txt}[t-1]$, are regarded as the renewed dialog history representations, symbolized as $\hat{\mathbf{E}}_h$. This approach not only curtails the input sequence length but also significantly reduces the perturbations from extraneous words.

3.3 Visual Encoder

3.3.1 Preprocessing

To achieve a profound extraction of object features from each frame in the video, we resort to the Faster R-CNN model, a renowned convolutional network model optimized for object detection tasks [37]–[39]. For our implementation, we draw inspiration from an existing state-of-the-art approach and use a pretrained version of Faster R-CNN⁵ that was trained on the Visual Genome dataset [14]. Given the richness of videos in terms of the number of frames (F) and the plethora of objects (O) within these frames, it becomes pertinent to incorporate these features into a singular dimension. Hence, we amalgamate these dimensions, giving rise to the feature representation, $\mathbf{E}'_v \in \mathbb{R}^{n_v \times 2048}$. Here, n_v is a composite dimension, essentially the product of the frame count and the number of objects, formulated as $n_v = F \times O$.

While extraction is a crucial step, the alignment of these extracted features with the textual embeddings (from the question, for instance) is of paramount importance. Features from disparate sources often reside in different dimensional spaces; thus, a mapping mechanism becomes vital to bring congruity between them. For the purpose of achieving this congruence, we integrate a linear layer, further enhanced with the ReLU activation function and layer normalization. This can be mathematically expressed as:

$$\mathbf{E}_v = \text{Norm}(\phi(f_v(\mathbf{E}'_v))), \quad (6)$$

where f_v acts as a fully connected layer, functioning as a transformational matrix. The ReLU activation function, symbolized by ϕ , introduces non-linearity, ensuring the model can learn more complex patterns. Layer normalization, denoted by $\text{Norm}(\cdot)$, scales and shifts the features to ensure they have a mean of zero and a standard deviation of one. The resultant feature set, post this alignment procedure, is represented as $\mathbf{E}_v \in \mathbb{R}^{n_v \times d}$.

3.3.2 Iterative Reasoning

For a comprehensive extraction of data related to the question Q_t from video V , we introduce a novel multimodal iterative reasoning network. This design prioritizes cyclical modality interactions, incrementally refining the data acquired. Both modalities converge into a weight matrix, described as:

$$\begin{cases} \mathbf{E} = \mathbf{E}_q || \mathbf{E}_v, \\ \mathbf{W} = \text{Softmax}(\mathbf{E}\mathbf{E}^T), \end{cases} \quad (7)$$

where $\mathbf{W} \in \mathbb{R}^{(n_q+n_v) \times (n_q+n_v)}$ representing the weight matrix and $||$ indicating concatenation. The matrix is divided into four specific sub-matrices, reflecting different weight components: $\mathbf{W}[:, n_q, : n_q]$ for question-question weight, $\mathbf{W}[:, n_q, n_q :]$ for question-video weight, $\mathbf{W}[n_q :, : n_q]$ for video-question weight, and $\mathbf{W}[n_q :, n_q :]$ for video-video weight.

We utilize four separate attention networks, each capturing distinct semantic information and enhancing the representation across different dimensions. To elucidate, the video-augmented question representations are derived as:

$$\begin{cases} \mathbf{E}_q^v = \mathbf{W}^O ||_{j=1}^J \text{head}_j, \\ \text{head}_j = \text{Attention}(\mathbf{E}_q \mathbf{W}_j^Q, \mathbf{E}_v \mathbf{W}_j^K, \mathbf{E}_v \mathbf{W}_j^V), \\ \text{Attention}(\mathbf{Q}, \mathbf{K}, \mathbf{V}) = \text{Softmax}\left(\frac{\mathbf{Q}\mathbf{K}^T}{\sqrt{d}}\right)\mathbf{V}, \end{cases} \quad (8)$$

where the weight matrices \mathbf{W}^O , \mathbf{W}_j^Q , \mathbf{W}_j^K , and \mathbf{W}_j^V are trainable parameters, and the hyperparameter d scales the dot product within the attention mechanism. The number of attention heads is depicted by J , while the video-enhanced question representations are illustrated by \mathbf{E}_q^v . Similarly, the self-enhanced question representations \mathbf{E}_q^q , question-enhanced video representations \mathbf{E}_v^q , and self-enhanced video representations \mathbf{E}_v^v are obtained through the same procedure.

Subsequently, we amalgamate intra- and inter-modality information to garner more comprehensive representations, as described by,

$$\begin{cases} \mathbf{E}_q^{vis} = \text{Sum}(\mathbf{W}[:, n_q, : n_q]) * \mathbf{E}_q^q + \text{Sum}(\mathbf{W}[:, n_q, n_q :]) * \mathbf{E}_q^v, \\ \hat{\mathbf{E}}_v = \text{Sum}(\mathbf{W}[n_q :, : n_q]) * \mathbf{E}_v^q + \text{Sum}(\mathbf{W}[n_q :, n_q :]) * \mathbf{E}_v^v, \end{cases} \quad (9)$$

where $\text{Sum}(\cdot)$ implies the summation function, and $\mathbf{E}_q^{vis} \in \mathbb{R}^{n_q \times d}$ and $\hat{\mathbf{E}}_v \in \mathbb{R}^{n_v \times d}$ represent the fused question and video representations, respectively.

We recognize that a singular interaction is inadequate to fully elucidate the complex semantic signals within videos. Hence, the described procedure can be cycled, iteratively refining the features. Specifically, \mathbf{E}_q^{vis} and $\hat{\mathbf{E}}_v$ are considered as new inputs in Eqn. (7) in the next iteration. Multiple iterations appear to foster more efficacious representations for both the question and the video content, thus enhancing the overall system performance. A detailed examination of this iterative process can be found in the Parameter Analysis section.

3.4 Generator

To deepen our understanding of inquiries, we introduce a neural architecture equipped with gating mechanisms. This architecture adeptly merges relevant information from

5. <https://github.com/peteanderson80/bottom-up-attention>.

TABLE 1

Performance comparison with the latest methods on the AVSD@DSTC7 dataset. The best results are highlighted in bold and the second in underline.

Method	Year	BLEU-1	BLEU-2	BLEU-3	BLEU-4	METEOR	ROUGE-L	CIDEr
Baseline [10]	2019	0.626	0.485	0.383	0.309	0.215	0.487	0.746
HMA [40]	2019	0.633	0.490	0.386	0.310	0.242	0.515	0.856
RMFF [41]	2019	0.636	0.510	0.417	0.345	0.224	0.505	0.877
EE-DMN [42]	2019	0.641	0.493	0.388	0.310	0.241	0.527	0.912
HAN [43]	2019	0.718	0.584	0.478	0.394	0.267	0.563	1.094
MTN [11]	2019	0.731	0.597	0.490	0.406	0.271	0.564	1.127
JMAN [44]	2020	0.667	0.521	0.413	0.334	0.239	0.533	0.941
MSTN [45]	2020	-	-	-	0.377	0.275	0.566	1.115
MTN-P [21]	2020	0.750	0.619	0.514	0.427	0.280	0.580	1.189
BiST [18]	2020	0.755	0.619	0.510	0.429	0.284	0.581	1.192
VGNMN [16]	2021	-	-	-	0.429	0.278	0.578	1.188
SCGA [14]	2021	0.745	0.622	0.517	0.430	0.285	0.578	1.201
VGD [22]	2020	0.750	0.621	0.516	0.433	0.283	0.581	1.196
PDC [15]	2021	0.770	<u>0.653</u>	0.539	0.449	0.292	0.606	1.295
RLM [12]	2021	0.765	0.643	0.543	0.459	0.294	0.606	1.308
T5RLM [23]	2022	0.767	0.644	0.542	<u>0.461</u>	0.296	0.608	1.311
JVIT [19]	2022	0.776	0.652	0.544	0.453	0.300	<u>0.614</u>	1.315
DialogMCF [20]	2023	<u>0.777</u>	<u>0.653</u>	<u>0.547</u>	0.457	0.306	0.613	1.352
ITR	-	0.782	0.655	0.552	0.469	<u>0.305</u>	0.619	<u>1.331</u>

both dialog history and visual contexts. Specifically, we leverage a dynamic gate regulated by the initial query embeddings \mathbf{E}_q , text-rich question representations \mathbf{E}_q^{txt} , and visual-infused question representations \mathbf{E}_q^{vis} . The formal representation is given as follows:

$$\mathbf{g} = \sigma(\mathbf{W}_g[\mathbf{E}_q \parallel \mathbf{E}_q^{txt} \parallel \mathbf{E}_q^{vis}]), \quad (10)$$

where $\mathbf{W}_g \in \mathbb{R}^{d \times 3d}$ signifies the learnable parameter matrix, the symbol \parallel represents concatenation, and σ is the Sigmoid function. The controlling vector $\mathbf{g} \in \mathbb{R}^{n_q \times d}$, comprising elements within the range of 0 and 1, dictates the inclusion of the necessary information, defined as,

$$\hat{\mathbf{E}}_q = \mathbf{g} \odot \mathbf{E}_q^{txt} + (\mathbf{1} - \mathbf{g}) \odot \mathbf{E}_q^{vis}, \quad (11)$$

where \odot is indicative of the element-wise product operation and $\hat{\mathbf{E}}_q$ denotes the ultimate question representation. This gating mechanism flexibly adjusts the influence of each modality during reasoning, ensuring a balanced and holistic query representation.

Building upon the methodology proposed by [15], we utilize the pre-trained GPT-2 model, recognized for its advanced text generation capabilities, as the backbone for our response generator. Specifically, the generator creates responses based on the representations of the video $\hat{\mathbf{E}}_v$, the caption \mathbf{E}_c , the dialog history $\hat{\mathbf{E}}_h$, and the posed question $\hat{\mathbf{E}}_q$. The combined input for the generator is structured as $\{\hat{\mathbf{E}}_v, [\text{SEP}], \mathbf{E}_c, [\text{SEP}], \hat{\mathbf{E}}_h, [\text{SEP}], \hat{\mathbf{E}}_q\}$. Utilizing several transformer layers, the probability of generating a response $A_t = \{w_1^a, w_2^a, \dots, w_{n_a}^a\}$ is derived as:

$$\begin{aligned} p(A_t | V, C, H, Q_t; \theta) &\approx p(A_t | \hat{\mathbf{E}}_v, \mathbf{E}_c, \hat{\mathbf{E}}_h, \hat{\mathbf{E}}_q; \theta) \\ &= \prod_{i=1}^{n_a} p(w_i^a | w_{<i}^a, \hat{\mathbf{E}}_v, \mathbf{E}_c, \hat{\mathbf{E}}_h, \hat{\mathbf{E}}_q), \end{aligned} \quad (12)$$

TABLE 2
Details of the benchmark datasets AVSD@DSTC7 and AVSD@DSTC8.

	Train	Valid	Test@DSTC7	Test@DSTC8
Dialogs	7,659	1,787	1,710	1,710
QA pairs	153,180	35,740	13,490	18,810
Words	1,450,754	339,006	110,252	162,226

where n_a denotes the count of words in the generated response and θ signifies the parameter of the response generator.

3.5 Optimization

To refine our optimization strategy, we focus on reducing the negative log-likelihood associated with the actual answer. Employing the Maximum Likelihood Estimation (MLE) criterion facilitates this. The formal expression for the loss is:

$$\mathcal{L}_{mle} = - \sum_{i=1}^{n_a} \log(p(w_i^a | w_{<i}^a, \hat{\mathbf{E}}_v, \mathbf{E}_c, \hat{\mathbf{E}}_h, \hat{\mathbf{E}}_q)). \quad (13)$$

4 EXPERIMENTS

4.1 Dataset

In evaluating our model, we used a benchmark dataset tailored for video-grounded dialog. Sourced from the Charades human-activity dataset [46], it captures authentic human interactions about video snippets. Two notable versions of this dataset exist: AVSD@DSTC7 [31] and AVSD@DSTC8 [32]. It contains 7,659 training dialogs, 1,787 for validation, and 1,710 each for DSTC7 and DSTC8 testing in the text generation task. Although both testing sets have the same number of dialogs, more nuanced utterance

TABLE 3

Performance comparison with the latest methods on the AVSD@DSTC8 dataset. The best results are highlighted in bold and the second in underline.

Method	Year	BLEU-1	BLEU-2	BLEU-3	BLEU-4	METEOR	ROUGE-L	CIDEr
Baseline [10]	2019	-	-	-	0.293	0.212	0.483	0.679
MTN [11]	2019	-	-	-	0.352	0.263	0.547	0.978
MDMN [47]	2020	-	-	-	0.296	0.214	0.496	0.761
JMAN [44]	2020	0.645	0.504	0.402	0.324	0.232	0.521	0.875
MSTN [45]	2020	-	-	-	0.385	0.270	0.564	1.073
MTN-P [21]	2020	0.701	0.587	0.494	0.419	0.263	0.564	1.097
STSGR [17]	2021	-	-	-	0.357	0.267	0.553	1.004
SCGA [14]	2021	0.711	0.593	0.497	0.416	0.276	0.566	1.123
RLM [12]	2021	0.746	0.626	0.528	0.445	0.286	0.598	1.240
T5RLM [23]	2022	0.749	0.631	0.529	0.445	0.290	0.600	1.263
JVIT [19]	2022	0.748	0.632	<u>0.536</u>	<u>0.456</u>	0.289	0.600	<u>1.268</u>
DialogMCF [20]	2023	<u>0.756</u>	<u>0.633</u>	0.532	0.449	<u>0.293</u>	<u>0.601</u>	1.253
ITR	-	0.762	0.641	0.543	0.460	0.298	0.607	1.285

comprehension as well as long-term history dependency capture is more critical in DSTC8 due to longer sentences. Each dialog, tied to a video, contains ten paired question-response utterances. Dataset specifics are detailed in Table 2.

4.2 Experimental Settings

4.2.1 Implementation Details

We trained our model for 20 epochs using the Adam optimizer. The learning rate was set at $4.5e-4$ and reduced tenfold between the 5-th and 10-th epochs. Configurations included a frame count (F) of 15, object number (O) of 6, and attention heads (J) of 3. We set the selection threshold (p) at 0.6 and iterated the reasoning network three times. The feature dimension (d) was 768, and batches were organized in sets of 32. During decoding, we employed a beam search with a width of 5, a sequence length capped at 20, and a length penalty of 0.2. Hyperparameters were optimized using a grid search on the validation set. Experiments were conducted using PyTorch on a single NVIDIA A100-PCIE-40GB GPU with CUDA 11.0.

4.2.2 Evaluation Metrics

We employed widely-accepted automatic evaluation measures for natural language synthesis⁶. These metrics include BLEU, METEOR, ROUGE-L, and CIDEr. They compare generated responses with ground truth by assessing word alignment and provide insights into fluency, context relevance, and expressive diversity of the produced dialogs.

4.3 Performance Comparison

We evaluated the performance of our proposed framework against several state-of-the-art benchmarks. This comparison includes generalized methodologies (*e.g.*, MTN [11], BiST [18], SCGA [14]), as well as GPT-based strategies (*e.g.*, PDC [15], RLM [12], T5RLM [23]) on the AVSD@DSTC7 and AVSD@DSTC8 benchmark datasets. The results for the AVSD@DSTC7 dataset are summarized in Table 1, with the following notable insights:

- Our model exhibited substantial improvements over earlier baselines such as HMA, RMFF, and EE-DMN, with metrics like CIDEr showing a boost from 0.856 (HMA) to 1.331 (Our model), highlighting the distinct advantages of our model.
- Models leveraging pretrained language constructs like GPT-2 (PDC, RLM, T5RLM, and JVIT) generally outperformed non-pretrained counterparts, confirming the efficacy of pretrained models in text generation.
- Our model surpassed all compared methods, achieving the highest scores across almost all evaluation metrics. This demonstrates its effective handling of the text generation task, with results such as a BLEU-4 score of 0.469, a 3.5% improvement over the next-best JVIT model.

The performance of our proposed framework, juxtaposed against several state-of-the-art methods on the AVSD@DSTC8 dataset, is delineated in Table 3. Key observations and insights drawn from the comparative results are as follows:

- Across most methods, there is a noticeable decrease in performance from AVSD@DSTC7 to AVSD@DSTC8, evidenced by metrics like BLEU-4, METEOR, ROUGE-L, and CIDEr. For example, the BLEU-4 score of RLM drops from 0.459 to 0.445. Similar trends are seen in models like MTN-P and SCGA. This drop might be attributed to differences in the datasets rather than solely the performance of the models.
- Our proposed model continues to excel, showing improvements across various evaluation metrics for the AVSD@DSTC8 benchmark. Specifically, our method outperforms DialogMCF by 2.4% and 2.5% for BLEU-4 and CIDEr, respectively. These results emphasize the robustness and capability of our designed framework.

In conclusion, our methodology maintains a consistent edge over other contenders on both AVSD@DSTC7 and AVSD@DSTC8 datasets. This dominance, mirrored across diverse evaluation metrics, accentuates the dexterity and resilience of our devised approach. In particular, the repeated attainment of pinnacle scores across a myriad of metrics underscores the holistic efficacy of our model.

6. <https://goo.su/xzkY>.

TABLE 4

Performance comparison among the variants of our model on the AVSD@DSTC7 dataset. The best results are highlighted in bold.

Method	BLEU-1	BLEU-2	BLEU-3	BLEU-4	METEOR	ROUGE-L	CIDEr
ITR	0.782	0.655	0.552	0.469	0.305	0.619	1.331
w/o textual encoder	0.774	0.644	0.539	0.455	0.299	0.612	1.289
w/o visual encoder	0.771	0.642	0.537	0.452	0.298	0.613	1.292
w/o gate mechanism	0.775	0.650	0.547	0.465	0.301	0.616	1.326
w/o GPT-2 decoder	0.760	0.636	0.528	0.441	0.287	0.603	1.229

TABLE 5

Performance comparison among the variants of different generation methods on the AVSD@DSTC7 dataset. The best results are highlighted in bold.

Method	BLEU-1	BLEU-2	BLEU-3	BLEU-4	METEOR	ROUGE-L	CIDEr
Greedy Search	0.756	0.619	0.509	0.422	0.294	0.598	1.241
Nucleus Sampling	0.695	0.534	0.417	0.328	0.262	0.539	0.981
Contrastive Search	0.773	0.641	0.534	0.443	0.299	0.604	1.299
Beam Search	0.782	0.655	0.552	0.469	0.305	0.619	1.331

4.4 Ablation Study

The goal of our ablation study is to critically evaluate the individual contribution of distinct modules within our ITR model. By strategically removing certain components, we can assess their significance in the holistic performance of our model. We designed four derivatives to accomplish this:

- **w/o textual encoder.** We bypassed the proposed textual encoder, relying solely on the original history features \mathbf{E}_h and question features \mathbf{E}_q^{vis} generated by the visual encoder, in lieu of the processed features $\hat{\mathbf{E}}_h$ and $\hat{\mathbf{E}}_q$.
- **w/o visual encoder.** In this configuration, the proposed visual encoder was omitted, and the initial feature \mathbf{E}_v and question feature \mathbf{E}_q^{txt} emanating from the textual encoder were directly inputted into the generator.
- **w/o gate mechanism.** Instead of employing gate fusion, we derived the final question representation $\hat{\mathbf{E}}_q$ through a single fully connected layer, expressed as:

$$\hat{\mathbf{E}}_q = \mathbf{W}_f[\mathbf{E}_q^{txt} || \mathbf{E}_q^{vis}] + \mathbf{b}, \quad (14)$$

where $\mathbf{W}_f \in \mathbb{R}^{d \times 2d}$ and \mathbf{b} symbolize the learnable parameter matrix and vector, respectively.

- **w/o GPT-2 decoder.** In this derivative, the GPT-2 decoder was supplanted with the LSTM-based autoregressive decoder that was previously utilized in [11].

Table 4 presents a meticulous evaluation of the ITR model against its various derivatives using the AVSD@DSTC7 dataset. The empirical findings from this analysis solidify the effectiveness of the ITR model, accentuating the significance of each constituent component within the architecture. We glean the following salient insights from the data:

- The w/o textual encoder variant, which omits the textual encoder, underperforms in comparison to the full-fledged ITR model. This underscores the criticality of dialog history in grasping the nuances and intent behind user queries.
- Omitting the visual encoder, as seen in the w/o visual encoder derivative, diminishes performance, illuminat-

ing the pivotal role that iterative reasoning holds in refining question and video representations.

- The model that bypasses the gate mechanism (w/o gate mechanism) delivers suboptimal results compared to the complete ITR. This result reinforces the efficiency of the gate mechanism in fusing cross-modal information.
- There is a marked performance dip in the w/o GPT-2 decoder variant, which is a testament to the instrumental edge that pre-trained language models like GPT-2 provide in handling downstream tasks.

Overall, this ablation study clearly demarcates the contribution of each module to the performance of our model, highlighting the robust design of the proposed ITR framework.

4.5 Decoding Methods

Table 5 furnishes an in-depth analysis of various decoding strategies deployed within the domain of multimodal dialog generation. A synopsis of our findings is delineated below:

- **Greedy Search.** While Greedy search that selects the most probable subsequent word in each instance exhibits laudable performance (BLEU-1 score of 0.756), its methodical nature can sometimes overlook globally coherent or intricate responses due to its short-sighted selection strategy.
- **Nucleus Sampling.** Posting a BLEU-1 score of 0.695, nucleus sampling amalgamates randomness by selecting from a subset of the most likely subsequent words. The infusion of diversity within responses, while a strength, might underpin its subdued coherence in comparison to its counterparts within video-anchored dialogs.
- **Contrastive Search.** Registering a commendable BLEU-1 score of 0.773, the contrastive modus operandi evaluates divergent options, possibly assisting in sifting through the subtleties of video-grounded retorts. Notwithstanding its edge over the first two, it could not surpass beam search in our assessment.
- **Beam Search.** Clinching the pinnacle with a BLEU-1 score of 0.782, beam search meticulously appraises

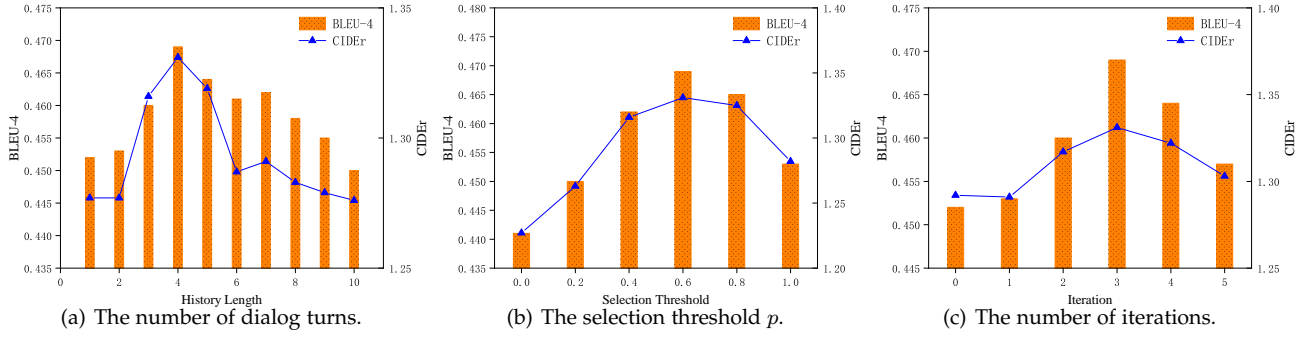


Fig. 4. Parameter analysis of our model in terms of the (a) the number of dialog turns, (b) the selection threshold p , (c) the number of iterations.

multiple trajectories during decoding, culminating in the selection of the most contextually rich sequence. Its supremacy across the board testifies to its aptness for tasks necessitating a precise grounding in stimuli like videos.

A salient feature of video-grounded dialog is its deterministic response modality, anchored firmly in the video and its captions. This deterministic nature diverges from the more fluid and open-ended nature of general open-domain dialogs. It’s evident, in light of this characteristic, that the beam search mechanism emerges as particularly adept for decoding tasks within this milieu.

4.6 Parameter Analysis

In this section, we delved deeper into the repercussions of three principal hyperparameters: the number of dialog turns, the selection threshold p , and the number of iterations in the ITR model.

4.6.1 On the number of dialog turns

Dialog turns in our model encapsulate the iterative interaction history, serving as a critical backdrop against which current interactions are contextualized. We embarked on a quest to discern the optimal number of dialog turns that our model should consider for peak performance.

As showcased in Figure 4(a), our experiments spanned dialog histories ranging from 1 to 10 turns. A discernible trend emerged: both the BLEU-4 and CIDEr metrics initially surged, peaking at a dialog history length of 4, before exhibiting a downturn. This oscillation underscores a salient feature: while history is undeniably beneficial, inundating the model with an overabundance of it seems counterproductive. The decline in performance with longer dialog histories hints at the introduction of noise or redundant information, which potentially obfuscates more pertinent recent interactions.

4.6.2 On the selection threshold p

The selection threshold p plays a pivotal role in filtering and modulating the information processed by the ITR model. To pinpoint its optimal value, we scrutinized the performance of our model across varying threshold levels.

The outcomes, illustrated in Figure 4(b), reveal a distinct pattern. The CIDEr metric, along with the BLEU-4 score, starts off with a surge, culminating in a peak at a threshold of 0.6, post which there is a decline. This showcases that extreme values on either end of the spectrum aren’t conducive.

While an extremely stringent threshold might deprive the model of necessary data, an overly lenient one might flood it with superfluous information.

4.6.3 On the number of iterations

The reasoning network, nested within the visual encoder, embarks on an iterative journey to refine its understanding of the given content. The question then arises: how many iterations strike the right balance between refinement and over-complication?

Our data, highlighted in Figure 4(c), offers an answer. Both BLEU-4 and CIDEr metrics register peak performances at three iterations, suggesting that this is the sweet spot. A deeper dive reveals that beyond this point, adding more iterations seems counterproductive. This could be attributed to the additional computational overhead and potential for overfitting that come with more iterations.

4.7 Case Study

Deep-diving into the applied implications of our ITR model, we present a series of case studies sourced from the AVSD@DSTC7 dataset. While quantitative evaluations provide insights into the overall performance of our model, case studies offer a qualitative lens to appreciate its nuanced behaviors and decision-making rationale. In Figure 5, we offer a visual manifestation of two exemplar cases: Case A and Case B. Each case elucidates the action of our model by illustrating the subject path and object path that the model opts to traverse en route to deriving the final response.

In Case A, our model demonstrates its competence in sifting through the dialog history, isolating the information salient to the current interaction. It illustrates how the model constructs a subject path that accurately reflects the central theme of the inquiry, as well as an object path that pinpoints the specifics the user is inquiring about. The concordance between these paths and the final response manifests the coherence and logic embedded within the operations of the model. The correct answer is derived by linking the information from the paths, showcasing the intelligent decision-making of our model. Moreover, the traceable path structure affirms the interpretability of the ITR model. This fosters a level of trust, as the operations within the model can be tracked and understood rather than being concealed as a “black box”.

Case B further reinforces the findings from Case A, highlighting the consistency in the performance of our model across diverse scenarios. Here too, the model meticulously

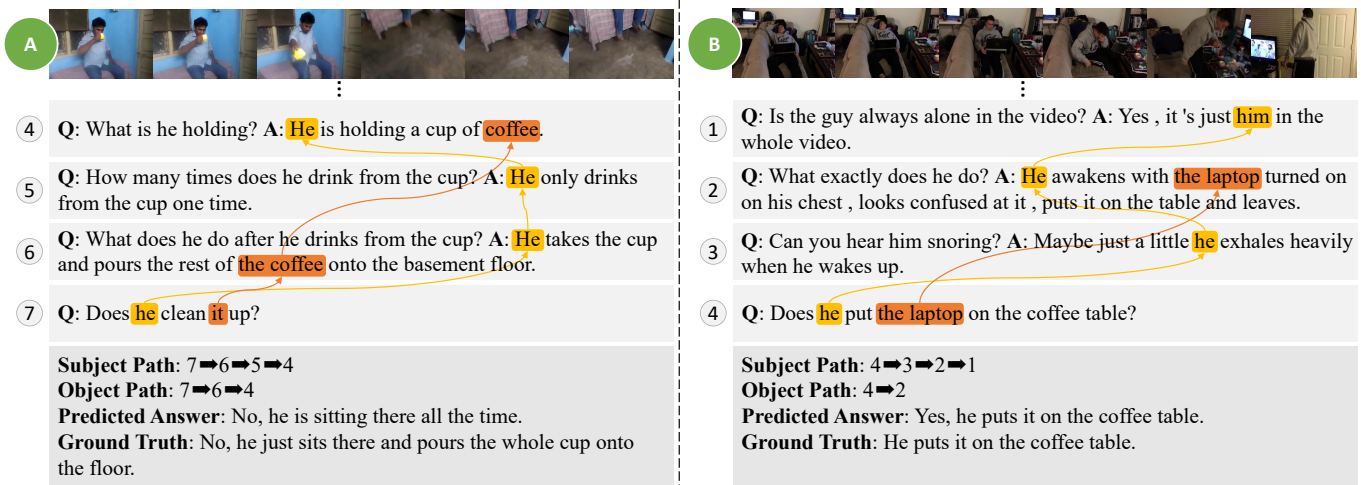


Fig. 5. Two visualization examples.

constructs paths that are reflective of the dialog history and the user's inquiry. The synthesis of these paths into an accurate answer once again illustrates the ability of our model to harness complex, multi-turn dialogs into coherent, precise responses. The systematic construction and the clear linkage between paths and answers in Case B underscore the robustness of the model and its potential to handle a wide array of real-world queries.

5 CONCLUSION AND FUTURE WORK

In this paper, we introduce the Iterative Tracking and Reasoning (ITR) framework tailored for video-grounded dialog. The ITR framework comprises three main components: a textual encoder, a visual encoder, and a generator. Our textual encoder is equipped with a path tracking and aggregation strategy, which meticulously aggregates context pertinent to the user's question, thus augmenting textual comprehension. In the visual domain, we introduce a multimodal iterative reasoning network within our visual encoder. This network delves deep into visual semantics that resonate with the user's inquiry, thereby bolstering visual understanding. Merging these enriched insights, we employ the pre-trained GPT-2 model as our response generator to craft the final response. Rigorous evaluations across two benchmark datasets vouch for the preeminence of our ITR model over prevailing techniques.

In the future, we intend to explore multimodal large language models, facilitating research in the field of video-grounded dialog. Besides, we also plan to study video-grounded dialog in more perspectives, *e.g.*, egocentric video dialog.

REFERENCES

- [1] H. Zhang, M. Liu, Z. Gao, X. Lei, Y. Wang, and L. Nie, "Multimodal dialog system: Relational graph-based context-aware question understanding," in *ACM MM*, 2021, pp. 695–703.
- [2] F. Liu, J. Liu, R. Hong, and H. Lu, "Question-guided erasing-based spatiotemporal attention learning for video question answering," *IEEE TNNLS*, vol. 34, no. 3, pp. 1367–1379, 2023.
- [3] C. Yin, J. Tang, Z. Xu, and Y. Wang, "Memory augmented deep recurrent neural network for video question answering," *IEEE TNNLS*, vol. 31, no. 9, pp. 3159–3167, 2020.
- [4] L. Li, J. Lei, Z. Gan, and J. Liu, "Adversarial vqa: A new benchmark for evaluating the robustness of vqa models," in *ICCV*, 2021, pp. 2042–2051.
- [5] Z. Yang, Z. Gan, J. Wang, X. Hu, Y. Lu, Z. Liu, and L. Wang, "An empirical study of gpt-3 for few-shot knowledge-based vqa," in *AAAI*, 2022, pp. 3081–3089.
- [6] D. Guo, H. Wang, and M. Wang, "Context-aware graph inference with knowledge distillation for visual dialog," *IEEE TPAMI*, vol. 44, no. 10, pp. 6056–6073, 2022.
- [7] C. Chen, Z. Tan, Q. Cheng, X. Jiang, Q. Liu, Y. Zhu, and X. Gu, "Utc: A unified transformer with inter-task contrastive learning for visual dialog," in *CVPR*, 2022, pp. 18 103–18 112.
- [8] P. H. Seo, A. Nagrani, A. Arnab, and C. Schmid, "End-to-end generative pretraining for multimodal video captioning," in *CVPR*, 2022, pp. 17 959–17 968.
- [9] K. Lin, L. Li, C.-C. Lin, F. Ahmed, Z. Gan, Z. Liu, Y. Lu, and L. Wang, "Swinbert: End-to-end transformers with sparse attention for video captioning," in *CVPR*, 2022, pp. 17 949–17 958.
- [10] C. Hori, H. Alamri, J. Wang, G. Wichern, T. Hori, A. Cherian, T. K. Marks, V. Cartillier, R. G. Lopes, A. Das *et al.*, "End-to-end audio visual scene-aware dialog using multimodal attention-based video features," in *ICASSP*, 2019, pp. 2352–2356.
- [11] H. Le, D. Sahoo, N. F. Chen, and S. C. Hoi, "Multimodal transformer networks for end-to-end video-grounded dialogue systems," in *ACL*, 2019, pp. 5612–5623.
- [12] Z. Li, Z. Li, J. Zhang, Y. Feng, and J. Zhou, "Bridging text and video: A universal multimodal transformer for audio-visual scene-aware dialog," *IEEE TASLP*, vol. 29, pp. 2476–2483, 2021.
- [13] B. Zhao, M. Gong, and X. Li, "Audiovisual video summarization," *IEEE TNNLS*, vol. 34, no. 8, pp. 5181–5188, 2023.
- [14] J. Kim, S. Yoon, D. Kim, and C. D. Yoo, "Structured co-reference graph attention for video-grounded dialogue," in *AAAI*, 2021, pp. 1789–1797.
- [15] H. Le, N. F. Chen, and S. C. Hoi, "Learning reasoning paths over semantic graphs for video-grounded dialogues," in *ICLR*, 2021.
- [16] H. Le, N. Chen, and S. Hoi, "Vgnmn: Video-grounded neural module networks for video-grounded dialogue systems," in *NAACL*, 2022, pp. 3377–3393.
- [17] S. Geng, P. Gao, M. Chatterjee, C. Hori, J. Le Roux, Y. Zhang, H. Li, and A. Cherian, "Dynamic graph representation learning for video dialog via multi-modal shuffled transformers," in *AAAI*, 2021, pp. 1415–1423.
- [18] H. Le, D. Sahoo, N. F. Chen, and S. C. Hoi, "Bist: Bi-directional spatio-temporal reasoning for video-grounded dialogues," in *EMNLP*, 2020, pp. 1846–1859.
- [19] H. Zhang, Y. Li, and Z. Zhang, "Video-grounded dialogues with joint video and image training," in *ICIP*, 2022, pp. 3903–3907.
- [20] Z. Chen, H. Liu, and Y. Wang, "Dialogmcf: Multimodal context flow for audio visual scene-aware dialog," *IEEE TASLP*, pp. 1–13, 2023.
- [21] H. Le and N. F. Chen, "Multimodal transformer with pointer network for the dstc8 avsd challenge," in *AAAI Workshop*, 2020.
- [22] H. Le and S. C. Hoi, "Video-grounded dialogues with pretrained generation language models," in *ACL*, 2020, pp. 5842–5848.

- [23] S. Yoon, E. Yoon, H. S. Yoon, J. Kim, and C. Yoo, "Information-theoretic text hallucination reduction for video-grounded dialogue," in *EMNLP*, 2022, pp. 4182–4193.
- [24] Y. Niu, H. Zhang, M. Zhang, J. Zhang, Z. Lu, and J.-R. Wen, "Recursive visual attention in visual dialog," in *CVPR*, 2019, pp. 6679–6688.
- [25] L. Yang, F. Meng, X. Liu, M.-K. D. Wu, V. Ying, and J. Xu, "Seqdial: Sequential visual dialog network in joint visual-linguistic representation space," in *AAAI Workshop*, 2021, pp. 8–17.
- [26] X. Zhao, L. Chen, and H. Chen, "A weighted heterogeneous graph-based dialog system," *IEEE TNNLS*, vol. 34, no. 8, pp. 5212–5217, 2023.
- [27] I. Schwartz, S. Yu, T. Hazan, and A. G. Schwing, "Factor graph attention," in *CVPR*, 2019, pp. 2039–2048.
- [28] D. Guo, H. Wang, H. Zhang, Z.-J. Zha, and M. Wang, "Iterative context-aware graph inference for visual dialog," in *CVPR*, 2020, pp. 10 055–10 064.
- [29] Y. Wang, S. Joty, M. Lyu, I. King, C. Xiong, and S. C. Hoi, "Vd-bert: A unified vision and dialog transformer with bert," in *EMNLP*, 2020, pp. 3325–3338.
- [30] V.-Q. Nguyen, M. Suganuma, and T. Okatani, "Efficient attention mechanism for visual dialog that can handle all the interactions between multiple inputs," in *ECCV*, 2020, pp. 223–240.
- [31] H. Alamri, C. Hori, T. K. Marks, D. Batra, and D. Parikh, "Audio visual scene-aware dialog (avsd) track for natural language generation in dstc7," in *AAAI Workshop*, 2018.
- [32] C. Hori, A. Cherian, T. Hori, and T. K. Marks, "Audio visual scene-aware dialog (avsd) track for natural language generation in dstc8," in *AAAI Workshop*, 2020.
- [33] X. Zhao, Y. Wang, C. Tao, C. Wang, and D. Zhao, "Collaborative reasoning on multi-modal semantic graphs for video-grounded dialogue generation," in *EMNLP Findings*, 2022, pp. 5988–5998.
- [34] H. Zhang, X. Li, and L. Bing, "Video-llama: An instruction-tuned audio-visual language model for video understanding," *arXiv preprint arXiv:2306.02858*, 2023.
- [35] B. Li, Y. Zhang, L. Chen, J. Wang, J. Yang, and Z. Liu, "Otter: A multi-modal model with in-context instruction tuning," *arXiv preprint arXiv:2305.03726*, 2023.
- [36] H. Zhang, M. Liu, Y. Li, M. Yan, Z. Gao, X. Chang, and L. Nie, "Attribute-guided collaborative learning for partial person re-identification," *IEEE TPAMI*, pp. 1–17, 2023.
- [37] S. Ren, K. He, R. Girshick, and J. Sun, "Faster r-cnn: Towards real-time object detection with region proposal networks," in *NeurIPS*, 2015, pp. 1–9.
- [38] Y. Yin, D. Xu, X. Wang, and L. Zhang, "Directional deep embedding and appearance learning for fast video object segmentation," *IEEE TNNLS*, vol. 33, no. 8, pp. 3884–3894, 2022.
- [39] G. Vecchio, S. Palazzo, D. Giordano, F. Rundo, and C. Spampinato, "Mask-rl: Multiagent video object segmentation framework through reinforcement learning," *IEEE TNNLS*, vol. 31, no. 12, pp. 5103–5115, 2020.
- [40] H. Le, S. Hoi, D. Sahoo, and N. Chen, "End-to-end multimodal dialog systems with hierarchical multimodal attention on video features," in *AAAI Workshop*, 2019.
- [41] Y.-T. Yeh, T.-C. Lin, H.-H. Cheng, Y.-H. Deng, S.-Y. Su, and Y.-N. Chen, "Reactive multi-stage feature fusion for multimodal dialogue modeling," in *AAAI Workshop*, 2019.
- [42] K.-Y. Lin, C.-C. Hsu, Y.-N. Chen, and L.-W. Ku, "Entropy-enhanced multimodal attention model for scene-aware dialogue generation," in *AAAI Workshop*, 2019.
- [43] R. Sanabria, S. Palaskar, and F. Metze, "Cmu sinbad's submission for the dstc7 avsd challenge," in *AAAI Workshop*, 2019.
- [44] Y.-W. Chu, K.-Y. Lin, C.-C. Hsu, and L.-W. Ku, "Multi-step joint-modality attention network for scene-aware dialogue system," in *AAAI Workshop*, 2020.
- [45] H. Lee, S. Yoon, F. Deroncourt, D. S. Kim, T. Bui, and K. Jung, "Dstc8-avsd: Multimodal semantic transformer network with retrieval style word generator," in *AAAI Workshop*, 2020.
- [46] G. A. Sigurdsson, G. Varol, X. Wang, A. Farhadi, I. Laptev, and A. Gupta, "Hollywood in homes: Crowdsourcing data collection for activity understanding," in *ECCV*, 2016, pp. 510–526.
- [47] H. Xie and I. Iacobacci, "Audio visual scene-aware dialog system using dynamic memory networks," in *AAAI Workshop*, 2020.